Lean NO_x trap study on a light-duty diesel engine using fast-response emission analysers

Alimin, A. , Benjamin, S.F. and Roberts, C.A.

Lean NO_X trap study on a light-duty diesel using fast response emission analysers

A.J. Alimin, S.F. Benjamin and C. A. Roberts

Automotive Engineering Applied Research Group, Coventry University, UK

Abstract

Storage and regeneration events have been studied using fast response emission analysers (~10ms) for a lean NOx trap fitted to a light-duty diesel engine. Tests were conducted at both low and high exhaust temperatures for various storage and purging periods. The use of fast response analysers has provided detailed information during the short regeneration periods and as combustion switched between rich and lean operating modes. It has also enabled quantification of the storage, reduction and overall conversion efficiencies as well as the instantaneous trapping efficiency. With exhaust temperatures of 250^{o}C storage efficiency was low ~30%. During purging two distinct NO spikes (breakthroughs) were measured downstream of the LNT at the beginning and end of regeneration. For this LNT the primary reducing mechanism is CO reacting with NO but CO reacting with ceria and/or water, the water-gas shift reaction, is suspected.. With exhaust temperatures of 400^{o}C storage efficiencies were high ~80-90% except for a case of long storage/short purge when the trap was near saturation. NOx breakthrough during enrichment depended on storage and purge periods and the availability of catalyst sites. NO_2 breakthrough was also observed at the end of regeneration as the combustion switched to lean operation. Generally, for the high temperature case on this LNT, the primary reducing mechanism is CO reacting with NO_2.

Keywords; lean NOx trap, catalyst, fast response emission analysers, aftertreatment, diesel

1 Introduction

Rising fuel costs and concerns regarding greenhouse gas emissions have resulted in an increase in the number of diesel passenger vehicles both in Europe and the US. The fuel economy improvement is due to the inherently better thermal efficiency of diesel over conventional petrol engines. However

diesels produce higher emissions of nitrogen oxides (NO_X) and particulates. Whilst technologies to deal with the latter are well advanced (particulate traps) reducing NOx is more problematic with the automotive industry facing tough challenges in order to comply with European and US emission regulations.

Conventional petrol engines operating at stoichiometric conditions with 3 way catalysts are extremely effective at reducing NOx. Diesels, however, burn with excess air and so reduction of NO_X to nitrogen in the exhaust gas stream is more difficult. European emission regulation Euro 4 (2005) requires NOx emissions limited to 0.25 g/km. Euro 5 (2009) and Euro 6 (2014) require further reductions to 0.18 and 0.08 g/km respectively. US standards are even more stringent with the current US Federal Tier 2 Bin 5 (2007) limits set at 0.044 g/km [**1**]. Whilst Euro 5 NOx emissions might be met with improvements in combustion technology it is almost certain that NOx after-treatment systems will be needed to meet Euro 6 and current US Federal Tier 2 Bin 5 regulations. The two main NOx after-treatment technologies under consideration are Lean NOx Traps (LNT) and Selective Catalytic Reduction (SCR). Each technology presents its own set of challenges and it is still uncertain which will prevail. Whilst both technologies have been demonstrated on engine test stands and in vehicles there is still a great deal of uncertainty as to the physical and chemical processes involved and so developing optimum design strategies is extremely challenging.

LNT catalysts typically use a blend of Pt/Rh- group metals, which catalyse the reduction/oxidation process and a basic adsorbent or base-metal-oxide (BMO) that provides the storage capacity. Typical adsorbers are barium oxide (BaO) and barium carbonate ($BaCO_3$). An oxidation catalyst converts engine-out NO emissions into NO_2. This is subsequently stored on the LNT during lean engine operation as NO_2 reacts with the BMO to form barium nitrate ($Ba(NO_3)_2$). Periodic regeneration of the trap under all driving condition is essential since it has a finite trapping capability. Regeneration is achieved by running the engine rich for a few seconds so that excess hydrocarbon (HC), carbon monoxide (CO) or hydrogen (H_2) reacts on the Pt/Rh group metals with the NOx that is released by disintegration of the nitrate under these conditions. The technology is challenging as LNTs are sulphur sensitive and only achieve highest conversion efficiencies within a limited temperature window. Other technical challenges relate to identifying the optimum storage/purging periods, preventing NOx

"slippage" during purging events and developing appropriate control strategies. In particular, too frequent purging provides a fuelling penalty whilst insufficient purging reduces trapping efficiency.

LNT behaviour has been studied in laboratory reactors using synthetic gases **[2-14],** on engine test beds **[9, 15-22]** and on vehicle drive cycle facilities **[8, 21, 22]**. Several research groups have developed mathematical models to describe LNT performance **[3, 16, 19, 21-25]**.This research has demonstrated that there are multifarious factors that can influence NO_X conversion efficiency amongst which are exhaust gas composition and temperature, air-fuel ratio, the duration of the lean and rich cycles and the composition of BMO and noble metal type. Epling [**26**] provides a useful summary and highlights a number of unresolved issues. One of these is the cause of NOx slippage around the time of transition from lean to rich conditions. NOx slippage, which reduces conversion efficiency, has been reported by many groups **[3, 6, 8-14, 17, 19, 20, 25]**.

The work described in this paper is part of a programme to develop a mathematical model of LNT systems for light-duty diesels **[16, 23]**.The model should be capable of describing both storage and purging events and be validated against engine test data. Most previous engine studies have been undertaken using emission analysers with response times of the order of seconds and therefore cannot provide the resolution to characterise trap behaviour during purging events. This paper addresses this issue by using fast-response emission analysers; the data generated will be used for model validation.

2 Experimental Test Rig

Figure 1 shows a schematic of the test rig and figure 2 the LNT system. In the experiments a 4-cylinder, 2 litre diesel engine was used, equipped with a common rail fuel injection system, exhaust gas recirculation (EGR) and an intake throttle body. The engine management system (EMS) comprised an engine control unit (ECU) and an injection control unit (ICU), and the throttle body was connected to the DSPACE control tool to enable periodic rich combustion. The EMS was also connected to a GREDI system that was used as the calibration tool for the engine. The fuel used throughout the tests was Carcal 55 low sulphur diesel (Swedish Class diesel).

The turbo outlet of the engine was linked to a lean NO_X trap test rig exhaust that consisted of a long diffuser followed by a flow straightener upstream of a DOC and an LNT. The diffuser and flow straightener therefore supplied approximately spatially uniform flow to the catalysts. The DOC used Pt as the main catalyst whilst the LNT used a blend of Pt and Rh. The LNT had a base metal oxide as the storage compound, supported by ceria.

The engine control software allowed control of the intake throttle body, EGR, as well as the injection quantities and timings for each of the pilot, main and post injections. It also produced different cyclic regeneration sets (alternating lean and rich operations). The in-cylinder enrichment technique was able to generate the rich combustion condition that was needed for regenerating the LNT. The approach used for in-cylinder enrichment in this study, which was based on varying fuel injection parameters and intake air throttling, was only one of many possible options for generating rich combustion but was used because it was the simplest. The fuel injection settings, amount and timing, were logged simultaneously at 50 Hz using GREDI. Data logging of emissions was performed at 50 Hz, using a Froude-Consine Texcel testbed data logger.

Fast response analysers (~10 ms) supplied by Cambustion were used to sample and analyse the exhaust emissions during storage and regeneration. An HFR500 Fast FID flame ionisation detector was used for sampling the HC emissions, a NDIR500 non-dispersive infra-red analyser for CO and CO_2 and a CLD500 chemiluminescence detector for NO and total NO_X. The sampling probe without a NO_X converter measured NO and with the converter measured total NO_X, thus allowing for measurement of NO_2 by subtraction. Each of the Cambustion instruments had two sampling heads and so at a given time six measurements could be made. Two wide band lambda sensors (Bosch lambda meter LA4 and lambda sensor LSU4.9) were used to record air fuel ratio and O_2 levels in the exhaust. Three separate gas sampling positions were chosen: inlet (before the DOC), gap (between the DOC and LNT) and outlet (after the LNT). Gas temperatures were measured upstream of the DOC, in the gap between the DOC and LNT and downstream of the LNT. The DOC and LNT brick temperatures were also measured at their centres. Emissions were sampled after engine and catalyst bed temperatures had approximately stabilised.

The fast response analysers captured details of the events during the storage and regeneration periods. The analysers were, in particular, able to measure the emissions traces during the rapid lambda changeover at the beginning and end of the regeneration period. The presence of signal noise in the emissions measurements was caused by small particles or carbon soot temporarily blocking the sampling passage from the probe heads to the service unit, see for example figure 3(b) between 72 and 122 s. The analysers became dirty in a very short time and required frequent meticulous cleaning. This limited the duration of each experiment. As it was not possible to simultaneously sample at all three sampling locations for all species composite plots were derived using data from different engine cycles. However in order to deduce the relative amounts of NO and NO_2 both NOx sampling heads were always placed at the same location. The data from each set of experiments were synchronised using the regeneration event (throttle body signal voltage) as the timing reference. Inevitably, however, there will be small differences between cycles.

Periodic storage and regeneration tests were carried out under conditions of steady speed and load. Measurements were taken when lean/purging events provided approximately cyclic behaviour from the LNT. Table 1 shows the test matrix which comprised various lean-storage/ rich-regeneration cycles and two different engine operating modes, A and B, designated as the low and high temperature conditions respectively.

3 Emissions test results

3.1 Low temperature study

(Engine Mode A: LT60L3R and LT60L6R)

These tests were performed at an exhaust temperature of about 250^{o}C at inlet to the test rig. The storage period was fixed at 60 seconds and two regeneration periods were examined, 3 and 6 seconds. This temperature is relatively low, leading to overall poor conversion efficiency. The cyclic NO, NO_2, HC, CO, CO_2, and O_2 plots during storage and regeneration for the LT60L3R test are shown in figures 3(a) – 3(f). For the HC emissions only the plots from the gap and outlet are presented

in figure 3(c). One regeneration for test LT60L3R is shown on an expanded scale in figures 4(a) and (b) and similarly for test LT60L6R in figures 5(a) and (b).

Figure 3 shows just two regenerations events. The cycle is repeated, and although there are some cycle to cycle variations, similar features were identified during each storage and regeneration event. Engine-out emissions show low levels of reductants, CO, HC during the lean or storage period. During the 3 second regeneration, CO and HC levels from the engine increase significantly whilst O_2 and NO_X levels fall. Figures 3(a) and (b) show NOx breakthrough occurring as two distinct NOx spikes recorded downstream of the LNT, either side of the regeneration event. During regeneration oxidation of CO across the LNT is observed; CO emissions post LNT are lower whereas CO_2 has increased, figs 3(d) and (e).

The NO_X emitted by the engine during the lean period was mostly NO which was partly oxidised to NO_2 by the DOC as evidenced by the increase of NO_2 and the decrease of NO across the DOC, figs 3(a) and (b). The reduction in NO_2 levels across the LNT shows that part is being stored, which is not the case for NO. Overall at this temperature the storage efficiency, discussed later, is poor.

Figures 4(a) and 5(a) show details during regeneration. The start of regeneration for these and subsequent figures can be deduced from when CO concentrations begin to rise at the first sampling location (inlet). The first NO breakthrough was generally much higher than the second. Increasing the regeneration period from 3-6 seconds did not have an effect on the NO_X breakthrough behaviour. The existence of NO_X spikes during regeneration has been noted by others, as noted earlier, but the fast response analysers have enabled the identification of two distinct events.

The first NOx release occurred as active purging of the trap began, and the storage compound $Ba(NO_3)_2$ started to disintegrate to NO which subsequently escaped the LNT before being reduced. Figures 4(a) and 5(a) show these NO spikes occurring between 64-65 secs and 67-68 secs respectively. CO after the trap was fully consumed during these time periods, figs 4(b) and 5(b), and the amount of CO_2 emitted increased correspondingly. However a molar balance analysis of NOx and CO **[27]** showed that significantly more CO was oxidised than required for NOx reduction over the

whole cycle. This suggests that CO oxidation was also occurring by other means. There is the possibility that ceria, oxidised during the lean storage phase, may be preferentially reduced by CO at the start of purging, equ (1).

$$CeO_2 + CO = Ce_2O_3 + CO_2 \quad (1)$$

The role of ceria during purges has been discussed by Theis **[8]**. Furthermore, under rich conditions, the water-gas shift (WGS) reaction **[19]** equ (2), may become important and might account for the rapid consumption of CO during the early part of regeneration. The liberation of H_2 from WGS may also contribute to the breakdown of $Ba(NO_3)_2$. It is interesting to note that recent publications **[19, 20]** have reported the formation of ammonia during purging which requires reaction with H_2

$$CO + H_2O \rightarrow CO_2 + H_2 \quad (2)$$

Following NO breakthrough figure 4(a) shows that between 65s and 66s no NO_X was observed post LNT. For the LT60L6R test, in figure 5(a), between 68s and 72s, NO_X was also absent. During these periods CO is partially consumed across the LNT, especially for the LT60L3R case, with CO_2 increasing. It is probable that stored NO has been released and has continued to react with a reductant, principally CO, catalysed by the Rh present on the LNT catalyst. The main function of Rh on an LNT catalyst is for assisting NO reduction by CO or HC [**11**]. At this point the rate limiting process is evidently NOx release rather than CO supply. HC was also consumed, fig3(c), but less so than CO, indicating that CO acts as the main reducing agent. This is consistent with the findings of West et al. **[18]**, as well as lab-scale studies on the role of CO by Abdulhamid et al. **[12]**.

Figure 4(a) shows a small secondary NOx spike appearing in the gap at the start of regeneration. A possible explanation for this is that some NOx is stored on the DOC during the lean period. During the lean period NOx levels post DOC were observed to be less than those upstream [**27**]. At the start of regeneration engine-out NOx levels are reduced and the resulting concentration gradient between the DOC and the exhaust gas stream causes a flux of NOx away from the surface of the DOC. A similar spike is seen in fig 5(a).

At the end of regeneration, the LT60L3R test, fig (4a), shows a spike of NO just before 67s within the gap and NO and NO_2 spikes post LNT. A similar breakthrough is observed for the LT60L6R test between 72 and 73s, see figure 5(a). The engine-out NO trace does not feature a sharp NO spike at this time thus suggesting the spike within the gap originates from the DOC and that post LNT from the LNT itself. This has not previously been reported.

The increase of CO_2 engine–out emissions during regeneration reflects the higher levels of EGR during this period. CO_2 post LNT is higher due to CO oxidation. At the end of regeneration figures 4(b) and 5(b) show spikes of CO_2 at all three locations, although they are higher post DOC and LNT indicating oxidation of any remaining CO, HC and carbonaceous material within the catalyst system as conditions become lean. Indeed temperatures were observed to increase in the DOC and LNT during regeneration [**27]**. Increasing the temperature of the LNT may reduce its storage capability perhaps triggering further NOx release. The NOx spike from the DOC may be due to carbonaceous material storing NOx during enrichment. As the mixture becomes lean this material is burnt off releasing NOx.

3.2 High Temperature (60 second storage)

(Engine Mode B: HT60L3R, HT60L6R and HT60L9R)

These tests were performed at an exhaust temperature of about 400 deg C at inlet to the test rig. The storage period was fixed at 60 seconds and three regeneration periods were examined, 3, 6 and 9 seconds. At this temperature higher conversion efficiency is expected. The cyclic NO, NO_2, CO, and CO_2, plots during storage and regeneration for the HT60L3R test are shown in figure 6(a) - (d). As with the tests at low temperature, emissions traces are similar from cycle to cycle. During the lean period the DOC oxidised some of the engine-out NO resulting in 50% of the NOx in the gap comprising NO_2. NOx from the DOC was stored completely by the LNT, as very low levels of NO and NO_2 were measured post LNT, figures 6(a) and (b). Moreover, there was no indication that the trap was starting to fill up, because the difference in level between the gap and the outlet remained large

50 s after a regeneration event. It is clear that operation at this high exhaust temperature improves the storage capability of the LNT.

CO and CO_2 emissions are shown in figures 6(c) and (d). They indicate full CO consumption inside the LNT during regeneration with CO_2 post LNT increasing significantly. CO consumption was also found to be much higher than HC consumption **[26]** suggesting that CO acts as the main reducing agent for trap regeneration and NO_X reduction at this higher temperature. Figure 6(b) shows NO_2 breakthrough towards the end of regeneration. The form of these NO_2 spikes varied between cases as discussed below.

The NO and NO_2 emissions at inlet, gap and outlet during regeneration for tests HT60L3R, HT60L6R and HT60L9R are shown respectively in figures 7(a), 8(a) and 9(a). The corresponding plots for CO and CO_2 are shown in figures 7(b), 8(b) and 9(b). Referring to the HT60L3R test, figure 7(a), between 63 and 64s, NO and NO_2 spikes were detected inside the gap as the lambda sensor registered the start of enrichment. The appearance of these spikes, as in the HT60L6R and HT60L9R tests in figures 8(a) and 9(a), could be explained as for the low temperature tests, i.e. NOx storage on the DOC during lean operation with release at the start of enrichment. Between 63 and 66s in figure 7(a), there was little NO or NO2 detected at the LNT outlet indicating reduction of released NOx. At 66 seconds however NO_2 is released i.e. 3 seconds from the start of the regeneration, whilst CO outlet is still zero. This suggests that release of NO_2 is faster than its reaction with CO at this time. It appears that almost the entire NO stored on the LNT has been released during purging as NO_2; with any NO being oxidised on Pt sites. The possibility of any reaction between CO and NO is discounted from a mole balance analysis [26]. It seems the released NO_2 fully consumes CO by catalysis as no CO was detected post LNT, fig 7(b). During the same time period, CO_2 emissions increase significantly after the LNT, fig 7(b). In contrast with the results from the low temperature tests the reaction between CO and NO_2 predominates. It seems that CO controls NO_2 release. Reaction between CO and NO_2 has been mentioned by others **[21, 22]**.

For the longer purges figures 8(a), 9(a) also show that around 2 -3 seconds from the start of regeneration NO_2 breakthrough was detected after the LNT. In figure 8(b) between 66 and 69s, and

figure 9(b), between 69 and 72s, the CO emission trace after the LNT shows complete consumption in the first 3 s into the regeneration period, and a large increase of CO_2 after the LNT. However between 68 and 72s in figure 8(a) and (b) and between 72 and 78s in figures 9(a) and (b), high levels of NO_2 and CO emissions are detected after the LNT. As CO emissions pre and post the LNT are similar it suggests that released NO_2 ceases to react with CO. One possible explanation is the lack of availability of Pt sites on the LNT. It appears that in the first 3 s of regeneration all the available Pt sites had been used up by the CO reacting with the NO_2. Clearly 3 seconds or slightly less would appear to be the optimum purge time for 60 seconds storage.

The occurrence of CO2 spikes in figures 7b, 8b, and 9b when the regeneration has ended may be explained as for the low temperature case, i.e. oxidation of remaining CO, HC and carbonaceous material during rich to lean transition. With reference to figure 7(a), between 66 and 67s a spike of NO_2 was observed (breakthrough) as the combustion mixture started to change from rich to lean. As in the case of the low temperature study this may be due to further release of NOx from the LNT due to the observed temperature rise in the LNT **[27].**

3.3 High Temperature (120 second storage)

(Engine Mode B: HT120L3R and HT120L9R)

High temperature tests were performed for longer storage (120 secs) and with purge times of 3 and 9 seconds. Emissions pre and post DOC and LNT, during regeneration for HT120L3R are shown respectively in figures 10(a) and (b). The plots for HT120L9R are displayed in figures 11(a) and (b).

In figures 10(a), around 123s, and 11(a), 129s, NO and NO_2 spikes were observed in the gap. The occurrence of these spikes could be explained as previously i.e. NOx storage on the DOC during lean operation with release at the start of enrichment.

For the longer storage and short regeneration test, HT120L3R, the trap was approaching saturation (see figure 13) and figure 10(a) shows that between 123 and 126s significant amounts of NO and NO_2

were therefore readily released; the reaction rate with CO being incapable of converting all.During the regeneration period, fig 10(b) shows CO had been fully consumed reacting with some of the released NOx.

With 9 sec purging, HT120L9R, figure 11(a) shows that between 129 and 138s very little NO emission was detected after the LNT compared with 3 sec purging, figure 10(a). This suggests more of the NO stored had been oxidised to NO_2 prior to $Ba(NO_3)_2$ decomposition. The NO_2 produced then reacted with CO, since between 129 and 134s CO was fully consumed and only started to rise after that when presumably the trap has been effectively purged. The CO_2 level post LNT for the HT120L9R test, shown in figure 11(b), increased as full consumption of CO was taking place. Some NO_2 breakthrough is observed as for the 3 sec purging test around 132-134 secs and gradually weakens or reacts halfway through the regeneration period, completely disappearing towards the end of the regeneration event. More NO_2 breakthrough occurred concurrently with CO consumption than was observed for the high temperature 60 second storage cases discussed earlier. For the longer 120 second storage period the trap is more saturated and thus NO2 release rate might be expected to more readily exceed the rate of reaction with CO. It would also seem that for 120 second storage only 5- 6 seconds of purging is required.

During the transition from rich to lean, between 126 and 127s for the HT120L3R test, figure 10(a), and between 138 and 140s for the HT120L9R test, figure 11(a) an NO_2 spike was observed after the LNT. Also as before, CO2 spikes are observed during rich to lean transition.

3.4 LNT system efficiency

It is instructive to compare the test cases in terms of conversion efficiencies. The LNT's performance is defined here with reference to its overall efficiency (storage and purging), trapping or storage efficiency, and reduction efficiency. If M_{in} and M_{out} are cumulative masses in and out of the LNT respectively and subscripts L and R refer to the lean and rich periods respectively then

$$\text{LNT Overall efficiency} = \frac{M_{\text{in L+R}} - M_{\text{out L+R}}}{} \qquad (4)$$

$$M_{in\ L+R}$$

$$\text{LNT Storage efficiency} = \frac{M_{in\ L} - M_{out\ L}}{M_{in\ L}} \qquad (5)$$

In equations (4) and (5), the lean and rich periods were defined respectively as the duration the engine was running in lean and rich conditions, as strictly indicated by the regeneration event of the intake air throttle.

$$\text{LNT Reduction efficiency} = \frac{\text{LNT Overall efficiency}}{\text{LNT Storage efficiency}} \qquad (6)$$

$$\text{Instantaneous NOx trapping efficiency} = \left[\frac{NOx_{in} - NOx_{out}}{NOx_{in}}\right] \times 100 \qquad (7)$$

In equation (7), NOx_{in} and NOx_{out} were the measured NO_X values (ppm) at the LNT inlet and outlet at each time instant. The plots for the LNT system instantaneous trapping efficiency as defined by equation (7) for the tests at low operating temperature are shown in figure 12(a), and the tests at high operating temperature are illustrated in figure 12(b) and 12(c). It can be seen that the instantaneous trapping efficiencies for both low temperature and high temperature groups start at low values due to the presence of NO_X spikes during the regeneration period.

Low temperature group tests operated at trapping efficiency between 20 – 70%. The trapping efficiency was highest immediately after regeneration before it began to drop gradually with time during the storage period. The situation is completely different with the high temperature group tests. Their trapping efficiencies were very high, between 85 – 98%, although under long storage and short regeneration, HT120L3R, the system trapping efficiency was lower, 40 – 70%. The lower instantaneous trapping efficiency for HT120L3R is ascribed to an insufficient regeneration period for purging the LNT.

The LNT system efficiencies - storage, overall and reduction- for all test conditions are summarised in figure 13. For the low temperature group, the storage, overall and reduction efficiencies at 6 s regeneration period were lower than regeneration at 3 s. Compared with the high temperature group, their storage and overall efficiencies are much lower, although the reduction efficiencies are comparable in both temperature groups. The highest storage, overall and reduction efficiencies were achieved in the HT60L3R and HT120L9R tests, where reduction efficiencies were nearly 100%. For tests using 60 s storage the overall system efficiency falls consistently as the regeneration period is increased, with 5 to 10 % change between experiments. For a longer storage period, 120 s, a significantly longer regeneration period is necessary to avoid saturating the trap.

3.5 Investigation of NO_X storage capacity

An investigation of the storage capacity of the LNT was performed by measuring the NO_X emissions pre and post LNT for an extended period of storage following a long regeneration period. In this experiment the engine was operated at 2000rpm/5bar, corresponding to the high temperature cases, and the regeneration period was 9 s. This would have fully purged the trap so that it was able to effectively store the incoming NO_X. Emissions were monitored until both the NO and NO_X measurements indicated saturation. Stored NO, NO_2 and NO_X based on cumulative mass are displayed in figure 14.

From figure 14, at around 16 minutes after regeneration there was no change in NO level across the LNT, so the trap was saturated with NO. Saturation for NO_2 occurred much later. After 28 minutes, NO_2 storage was still occurring, but the trap was approaching saturation. Clearly the LNT stores both NO and NO_2, although it adsorbs more NO_2.

4 Conclusions

Storage and regeneration events have been studied using fast response emission analysers (~10ms) for a lean NOx trap fitted to a light-duty diesel. Tests were conducted at both low and high exhaust temperatures for varying storage and purging periods. The use of fast response analysers has

provided detailed information during the short regeneration periods and as combustion switched between rich and lean operating modes thus providing a unique data base for on-going model validation. It has also enabled quantification of the storage, reduction and overall conversion efficiencies as well as the instantaneous trapping efficiency. The main conclusions are summarised below.

4.1 Low temperature

Tests were conducted for a 60 second storage period and with 3 and 6 sec purging.

- At an exhaust temperature of 250 deg C the storage efficiency was low, ~30%, with the instantaneous efficiency dropping from 70% to 20% as the trap filled. Reduction efficiencies during purging were ~80% resulting in low overall conversion efficiencies of about 25%.

- During purging two distinct NO spikes (breakthroughs) were measured downstream of the LNT at the beginning and end of regeneration.

- The first breakthrough originated from the LNT and is thought to be due to a combination of effects. At low temperature CO reduction with NO may be proceeding at a rate much slower than NO release from the BMO but CO preferably reacting with ceria and/or water, the water-gas shift reaction, is suspected.

- The second NO breakthrough observed during transition from rich to lean conditions may be associated with the reduction in storage capacity as the LNT temperature increased.

- Doubling the purging period from 3 to 6 seconds did not change the characteristics of NO breakthrough.

- The primary reducing mechanism for this LNT is CO, rather than HC, acting on NO.

4.2 High temperature

Tests were conducted for two storage periods, 60 and 120 secs. For the shorter storage, purge times of 3, 6 and 9 seconds were investigated whilst for the longer storage purging of 3 and 9 secs duration was used.

- At an exhaust temperature of 400 deg C the storage efficiencies were high, between 82-92%, except for the long storage/short purge case which showed a drop in efficiency as the trap filled. During purges reduction efficiencies were between 90 and 98% for all cases. Overall conversion efficiencies were generally high, between 74-90%, except for the long duration/short purge which was low at 40%.

- With 60 sec storage no substantial NOx breakthrough occurred with a 3 sec purge. For longer purges of 6 and 9 seconds NO_2 breakthrough was observed 2-3 seconds from the beginning of and up to the end of regeneration. This would seem to be a result of the unavailability of catalyst sites as little CO was consumed during this time. NO_2 breakthrough was also observed at the end of regeneration, as the combustion switched to lean operation and, as in the low temperature case, is possibly due to a reduction in storage capacity..

- For the 120 sec storage with 3 sec purge significant NO and NO_2 breakthrough occurred during purging as the trap was almost saturated. NOx breakthrough with the longer purge was less. NO_2 breakthrough was also observed at the end of regeneration as the combustion switched to lean operation.

- Generally for the high temperature case with this LNT the primary reducing mechanism is CO acting on NO_2 as distinct from that for low temperature.

Acknowledgments

The authors would like to thank Emcon Technologies, Jaguar Land Rover, Johnson Matthey and the Ford Motor Company, for their technical and financial support. Financial support from UTHM (Malaysia) to A. J. Alimin is gratefully acknowledged. We would also like to thank Stefan Hackenberg from ArvinMeritor and Robert Brisley from Johnson Matthey for helpful discussion.

References

1. www.dieselnet.com
2. **Epling, W. S., Parks, J. E., Campbell, G. C., Yezerets, A., Currier, N. W.** and **Campbell, L. E.** Further evidence of multiple NO_X sorption sites on NO_X storage/reduction catalysts, *Catalysis Today*, 2004, **96**, 21-30,
3. **Olsson, L., Fridell, E., Skoglundh, M.** and **Andersson, B.** Mean field modelling of NO_X storage on Pt/BaO/Al_2O_3, *Catalysis Today*, 2002, **73**, 263-270
4. **Takahashi, N., Shinjoh, H., Iijima, T., Suzuki, T., Yamazaki, K., Yokota, K., Suzuki, H., Miyoshi, N., Matsumoto, S., Tanizawa, T., Tanak, T., Tateishi, S.** and **Kasahara, K** The new concept 3-way catalyst for automotive lean-burn engine: NO_X storage and reduction catalyst, 1996, *Catalysis Today*, **27**, 63-69
5. **Kobayashi, T., Yamada, T.** and **Kayano, K.** Study of NO_X Trap Reaction by Thermodynamic Calculation, SAE paper 970745, 1997
6. **Fridell, E., Skoglundh, M., Westerberg, B., Johansson, S.** and **Smedler, G.** NO_X Storage in Barium-Containing Catalysts, 1999 *Journal of Catalysis*, **183**, 196-209
7. **Mahzoul, H., Brilhac, J.F. and Gilot, P.** (1999) Experimental and mechanistic study on NO_X adsorption over NO_X trap catalysts, *Applied Catalysis B: Environmental*, 1999 **20**, 47-55
8. **Theis, J. R., Ura, J. A., Li, J. J., Surnilla, G.G., Roth, J. M.** and **Goralski Jr., C. T.** NO_X Release Characteristics of Lean NO_X Traps during Rich Purges, SAE paper 2003-01-1159, 2003
9. **Bögner, W., Krämer, M., Krutzsch, B., Pischinger, S., Voigtländer, D., Wenninger, G., Wirbeleit, F., Brogan, M.S., Brisley, R.J.** and **Webster, D.E.** Removal of nitrogen oxides

from the exhaust of a lean-tune gasoline engine, 1995 *Applied Catalysis B: Environmental,* **7**, 153-171.

10. **Liu, Z.** and **Anderson, J. A.** Influence of reductant on the thermal stability of stored NO_X in $Pt/Ba/Al_2O_3$ NO_X storage and reduction traps, 2004 *Journal of Catalysis*, **224**, 18-27
11. **Amberntsson, A., Fridell, E.** and **Skoglundh, M.** Influence of platinum and rhodium on the NO_X storage and sulphur tolerance of a barium based NO_X storage catalyst, 2003 *Applied Catalysis B: Environmental*, **46**, 429-439
12. **Abdulhamid, H., Fridell, E.** and **Skoglundh, M.** The reduction phase in NO_X storage catalysis: Effect of type of precious metal and reducing agent, 2005 *Applied Catalysis B: Environmental*, **62**, 319-328
13. **Nova, I., Castoldi, L., Lietti, L., Tronconi, E.** and **Forzatti, P.** On the dynamic behaviour of "NO_X-storage/reduction" $Pt-Ba/Al_2O_3$ catalyst, 2002 *Catalysis Today*, **75**, 431-437
14. **James, D., Fourré, E., Ishii, M.** and **Bowker, M.** Catalytic decomposition/regeneration of $Pt/Ba(NO_3)_2$ catalysts: NO_X storage and reduction, 2003 *Applied Catalysis B: Environmental*, **45**, 147-159
15. **Fang, H., Huang, S. C., Yu, R. C., Wan, C.Z.** and **Howden, K.** A Fundamental Consideration on NO_X Adsorber Technology for DI Diesel Application, SAE paper 2002-01-2889, 2002
16. **Alimin A. J., Roberts C. A.,**and **Benjamin S. F.** A NO_X Trap Study using Fast Response Emission Analysers for Model Validation SAE paper 2006-01-0685, (also SP-2023), 2006
17. **Li, Y., Roth, S., Yassine, M., Beutel, T., Dettling, J.** and **Sammer, C.** Study of Factors Influencing the Performance of A NO_X Trap in a Light-Duty Diesel Vehicle, SAE paper 2000-01-2911, 2000
18. **West, B., Huff, S., Parks, J., Lewis, S., Choi, J-S., Partridge, W.** and **Storey, J.** Assessing Reductant Chemistry During In-Cylinder Regeneration of Diesel Lean NO_X Traps, SAE paper 2004-01-3023, 2004.
19. **Depcik, C., Assanis, D.** and **Bevan, K.** A one-dimensional lean NOx trap model with a global kinetic mechanism that includes NH_3 and N_2O 2008 *Int J Engine Res* **9** 57-77
20. **Hackenberg, S** and **Ranalli M.** Ammonia on a LNT: Avoid the Formation or Take Advantage of It SAE paper 2007-01-1239 (also SP-2080), 2007

21. **Hepburn, J., Kenney, T., McKenzie, J., Thanasiu, E. and Dearth, M.** Engine and aftertreatment modelling for gasoline direct injection, SAE paper 982596, 1998

22. **Ketfi-Cherif, A., Wissel, D. von., Beurthey, S.** and **Sorine, M.**Modelling and control of a NO_X trap catalyst, SAE paper 2000-01-1199, 2000

23. **Benjamin S. F.** and **Roberts C. A.** 3D modelling of NOx and particulate traps using CFD: a porous medium approach 2007 *Journal of Applied Mathematical Modelling* **31**/11 2446-2460

24. **Lauren, F., Pope C. J., Mahzoul, L., Delfosse L.** and **Gilot P.** Modelling of NOx absorption over NOx adsorbers. 2003 *Chem Eng Sci* **58** 1793-1803

25. **Margaritis N. K., Haralampous O. A.** and **Koltsakis G. C.** Modeling of the NOx trap and experimental validation using ultra-fast NOx analyzers 2007 *Topics in Catalysis* **42-43** 65-69.

26. **Epling W. S., Campbell L. E., Yezerets A., Currier N. W.** and **Parks II J. E**. Overview of the Fundamental Reactions and Degradation Mechanisms of NOx Storage/Reduction Catalysts. 2004 *Catalysis Reviews* **46** No 2 163-245

27. **Alimin A. J.** Experimental Investigation of a NOx trap using fast response emission analysers. PhD thesis, Coventry University 2006

List of Captions

Table 1

LNT storage and regeneration tests matrix

Figure 1

Schematic of the system set-up

Figure 2

Details of the LNT test rig

Figure 3a

LT60L3R-NO emissions during storage and regeneration

Figure 3b

LT60L3R-NO_2 emissions during storage and regeneration

Figure 3c

LT60L3R-HC emissions during storage and regeneration

Figure 3d

LT60L3R-CO emissions during storage and regeneration

Figure 3e

LT60L3R-CO_2 emissions during storage and regeneration

Figure 3f

LT60L3R-O_2 emissions during storage and regeneration

Figure 4a

LT60L3R-NO and NO_2 emissions during LNT regeneration

Figure 4b

LT60L3R-CO and CO_2 emissions during LNT regeneration

Figure 5a

LT60L6R-NO and NO_2 emissions during LNT regeneration

Figure 5b

LT60L6R-CO and CO_2 emissions during LNT regeneration

Figure 6a

HT60L3R-NO emissions during storage and regeneration

Figure 6b

HT60L3R-NO_2 emissions during storage and regeneration

Figure 6c

HT60L3R-CO emissions during storage and regeneration

Figure 6d

HT60L3R-CO_2 emissions during storage and regeneration

Figure 7a

HT60L3R-NO and NO_2 emissions during LNT regeneration

Figure 7b

HT60L3R-CO and CO_2 emissions during LNT regeneration

Figure 8a

HT60L6R-NO and NO_2 emissions during LNT regeneration

Figure 8b

HT60L6R-CO and CO_2 emissions during LNT regeneration

Figure 9a

HT60L9R-NO and NO_2 emissions during LNT regeneration

Figure 9b

HT60L9R-CO and CO_2 emissions during LNT regeneration

Figure 10a

HT120L3R-NO and NO_2 emissions during LNT regeneration

Figure 10b

HT120L3R-CO and CO_2 emissions during LNT regeneration

Figure 11a

HT120L9R-NO and NO_2 emissions during LNT regeneration

Figure 11b

HT120L9R-CO and CO_2 emissions during LNT regeneration

Figure 12(a)

LNT system instantaneous trapping efficiency for low operating temperature: LT60L3R and LT60L6R

Figure 12(b)

LNT system instantaneous trapping efficiency for high operating temperature: HT60L3R and HT60L6R and HT60L9R

Figure 12(c)

LNT system instantaneous trapping efficiency for high operating temperature: HT120L3R and HT120L9R

Figure 13

LNT system: Storage, overall and reduction efficiencies under different test conditions.

Figure 14:

NOx storage following LNT regeneration at high exhaust temperature.

Table 1: LNT storage and regeneration tests matrix

No.	Test name	Mode	Engine speed (RPM)	Torque (Nm)	Storage period (s)	Regeneration period (s)	Average exhaust temperatures at inlet (^{O}C)
1	LT60L3R	A	1500	48	60	3	241
2	LT60L6R	A	1500	48	60	6	249
3	HT60L3R	B	2000	80	60	3	387
4	HT60L6R	B	2000	80	60	6	402
5	HT60L9R	B	2000	80	60	9	394
6	HT120L3R	B	2000	80	120	3	382
7	HT120L9R	B	2000	80	120	9	395

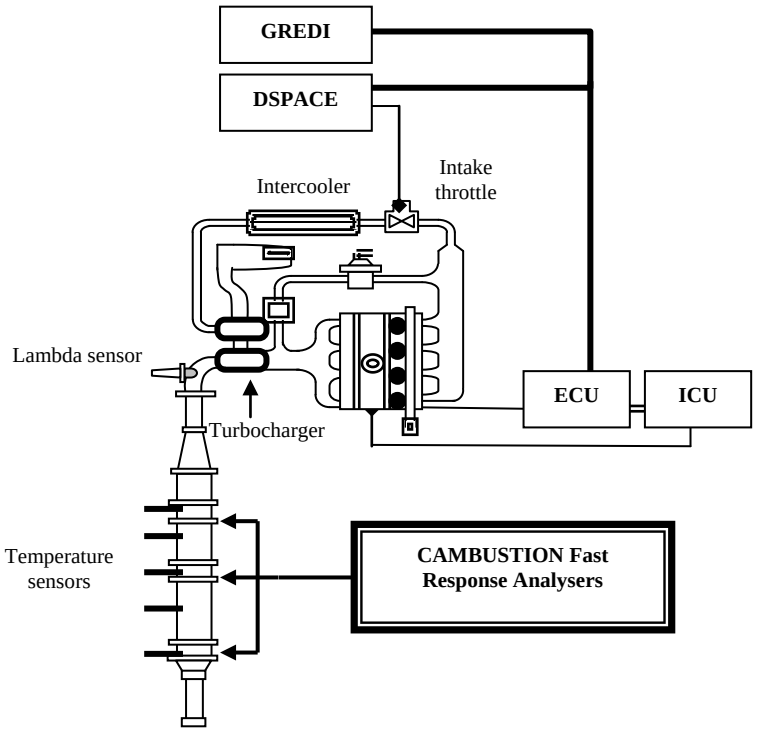

Figure 1: Schematic of the system set-up

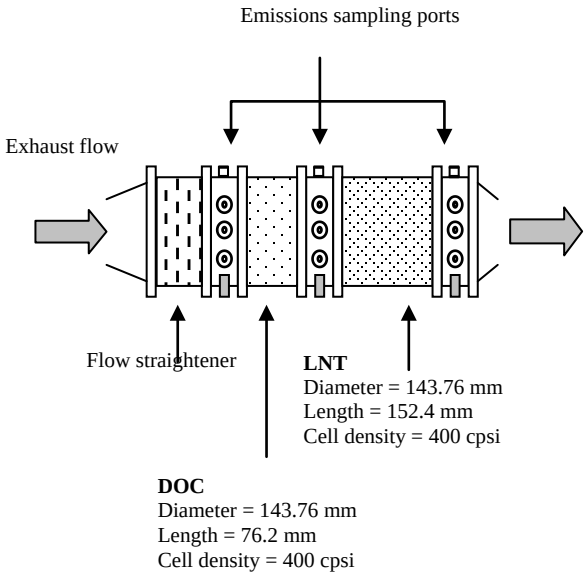

Figure 2: Details of the LNT test rig

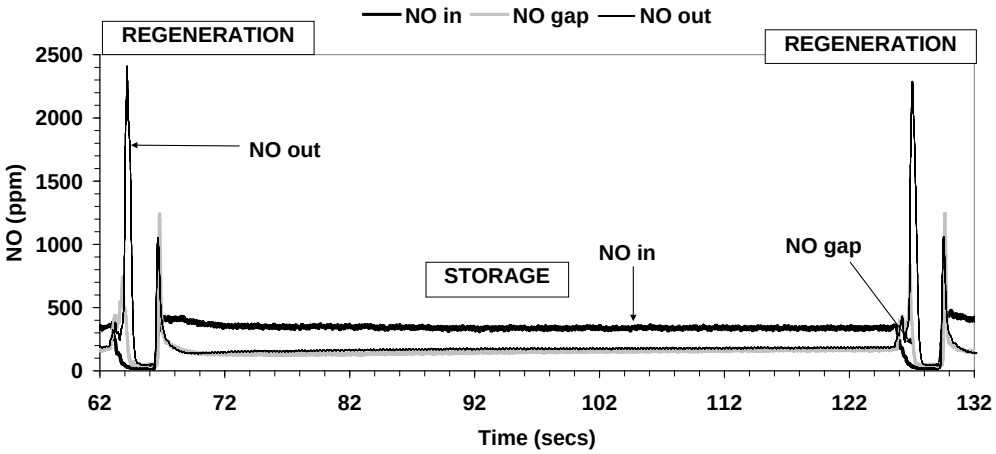

Figure 3(a): LT60L3R – NO emissions during storage and regeneration

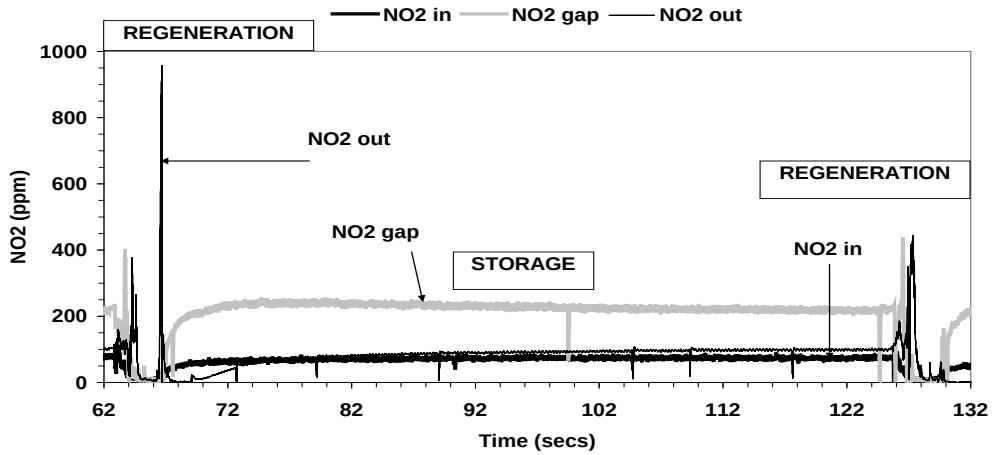

Figure 3(b): LT60L3R – NO_2 emissions during storage and regeneration

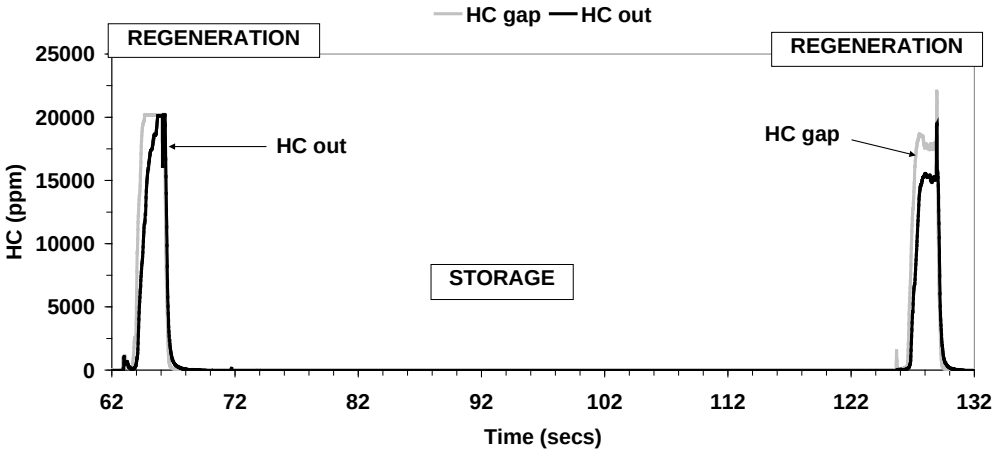

Figure 3(c): LT60L3R – HC emissions during storage and regeneration

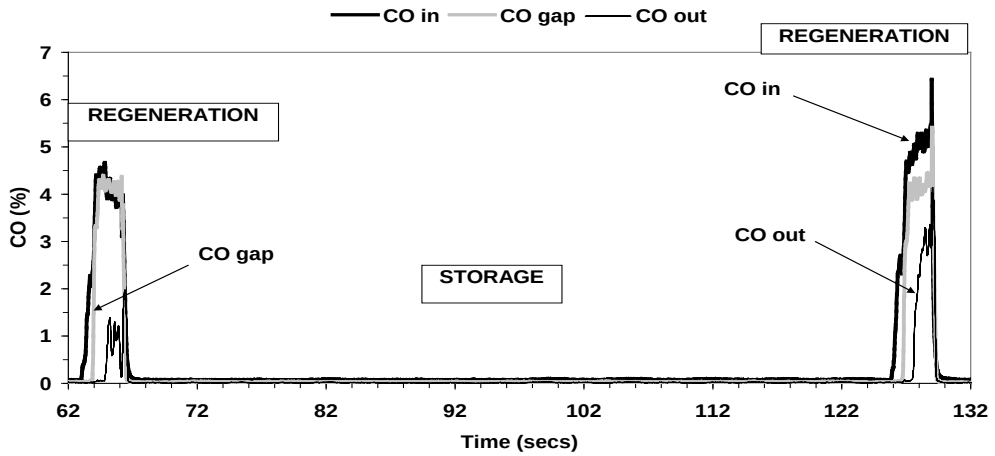

Figure 3(d): LT60L3R – CO emissions during storage and regeneration

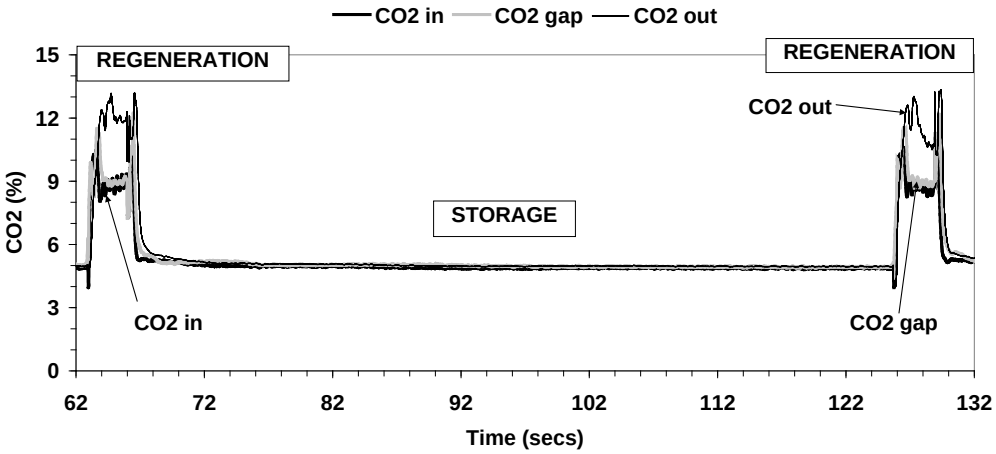

Figure 3(e): LT60L3R – CO_2 emissions during storage and regeneration

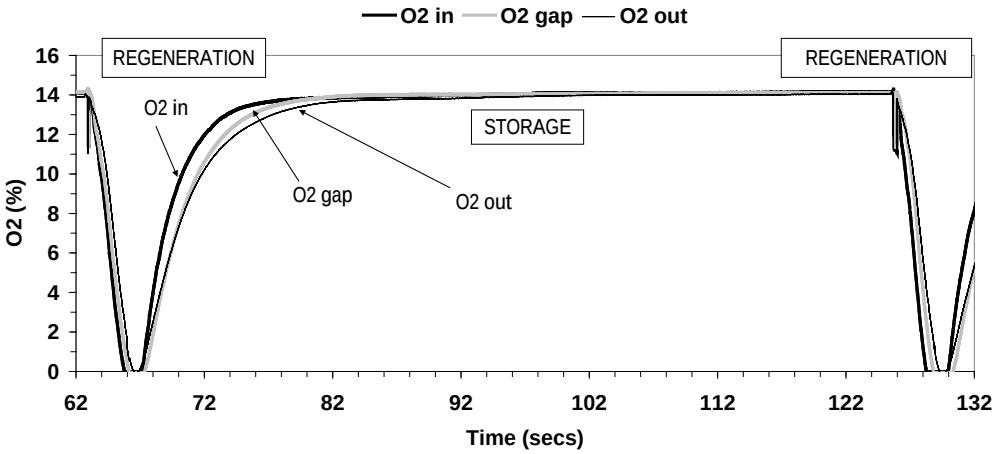

Figure 3(f): LT60L3R – O_2 emissions during storage and regeneration

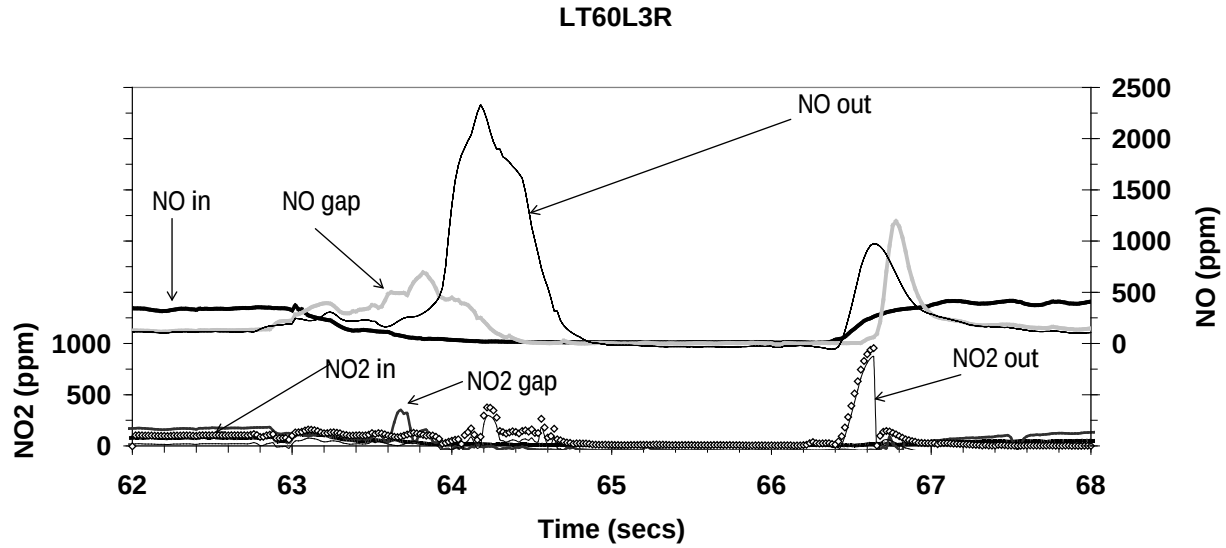

Figure 4(a): LT60L3R – NO and NO_2 emissions during LNT regeneration

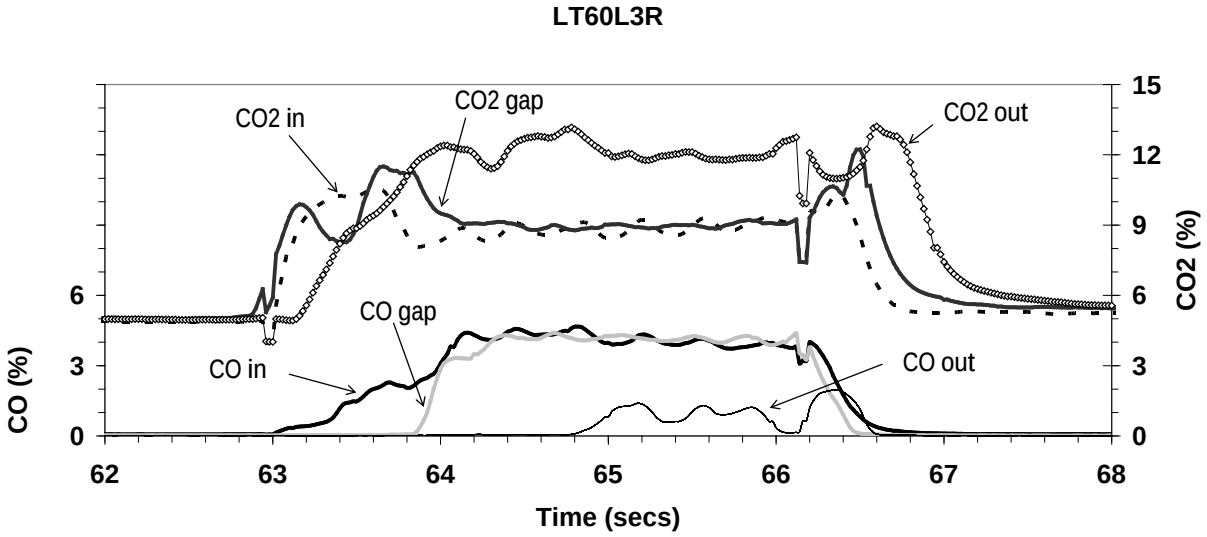

Figure 4(b): LT60L3R – CO and CO_2 emissions during LNT regeneration

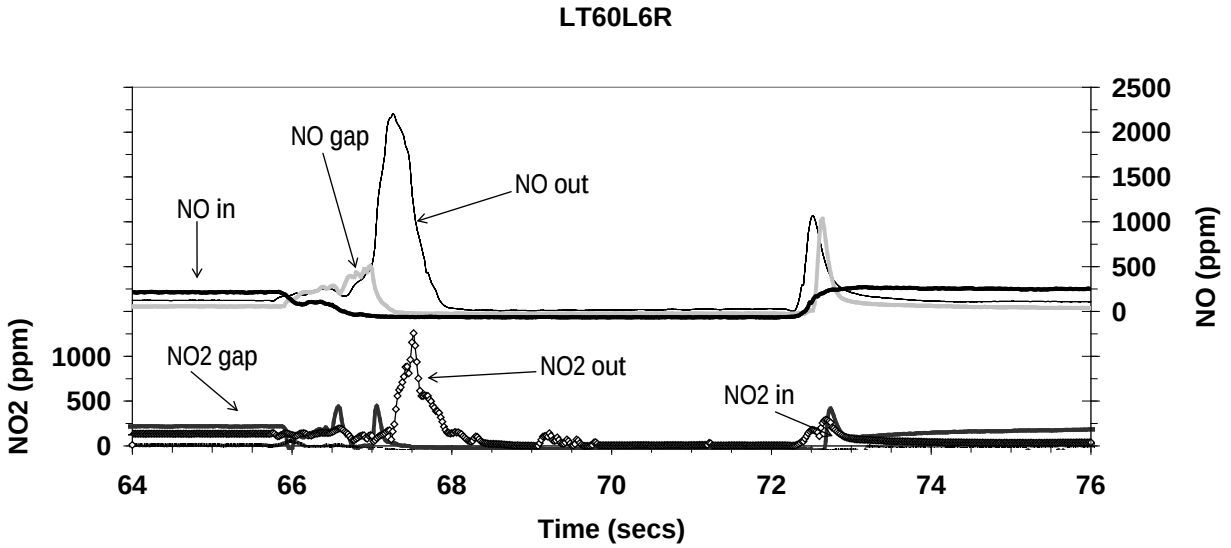

Figure 5(a): LT60L6R – NO and NO_2 emissions during LNT regeneration

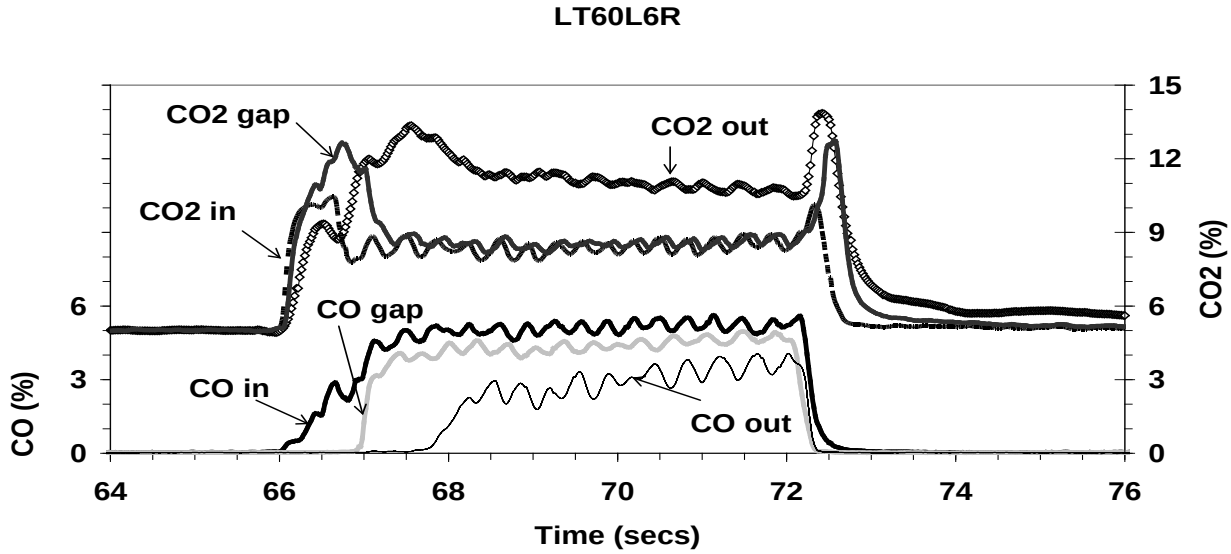

Figure 5(b): LT60L6R – CO and CO_2 emissions during LNT regeneration

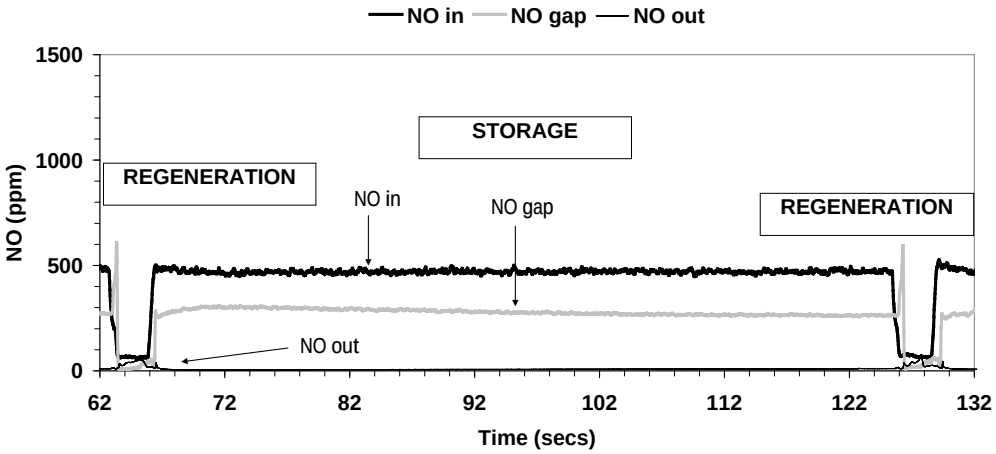

Figure 6(a): HT60L3R – NO emissions during storage and regeneration

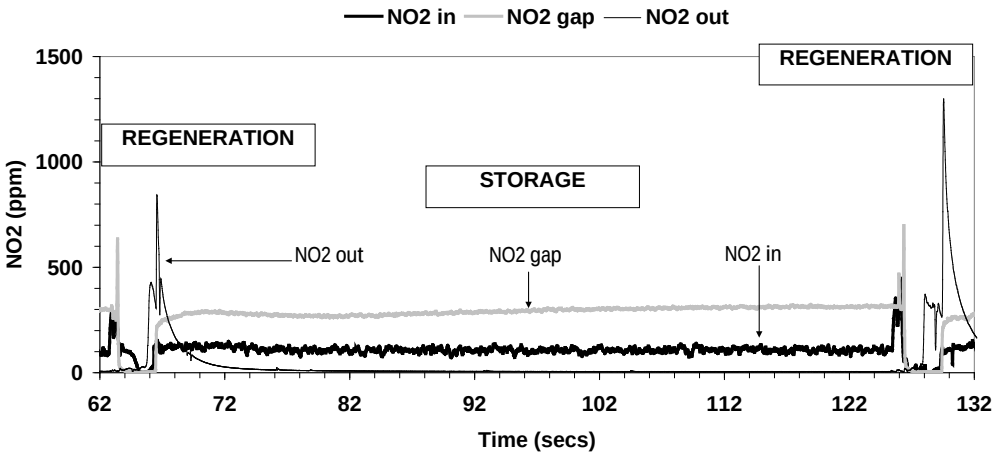

Figure 6(b): HT60L3R – NO_2 emissions during storage and regeneration

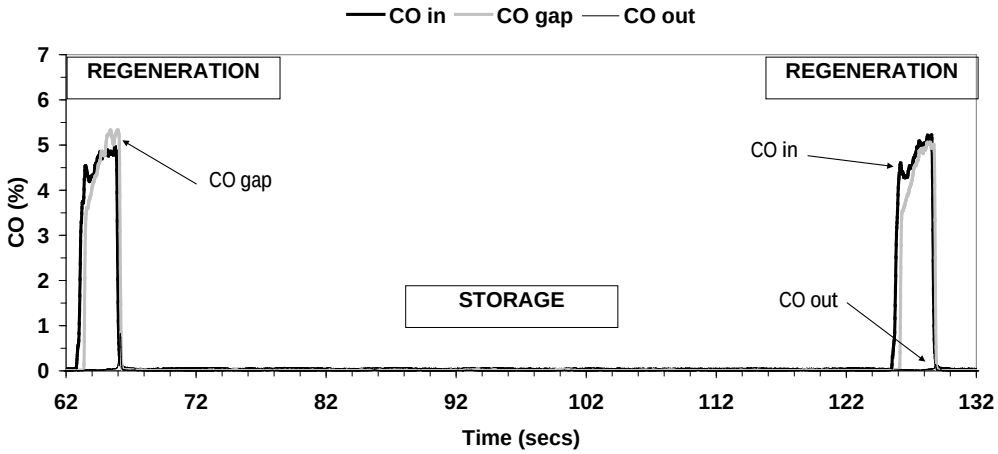

Figure 6(c): HT60L3R – CO emissions during storage and regeneration

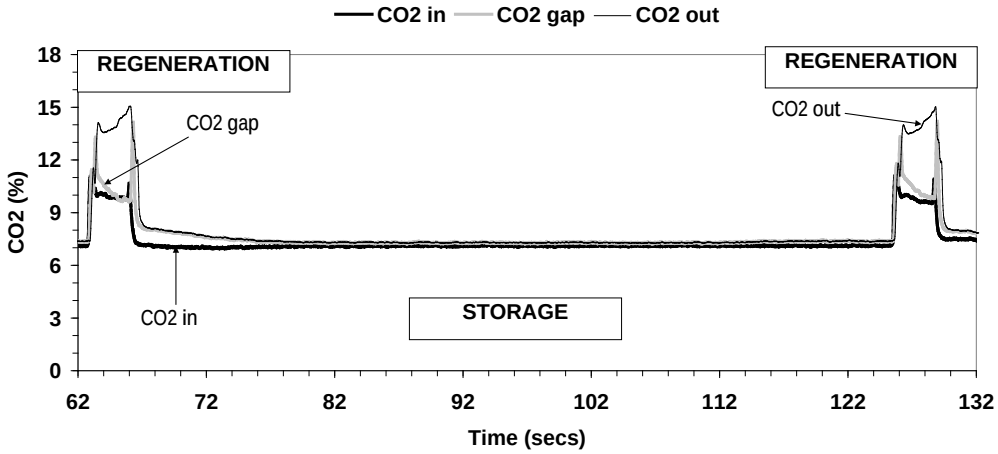

Figure 6(d): HT60L3R – CO_2 emissions during storage and regeneration

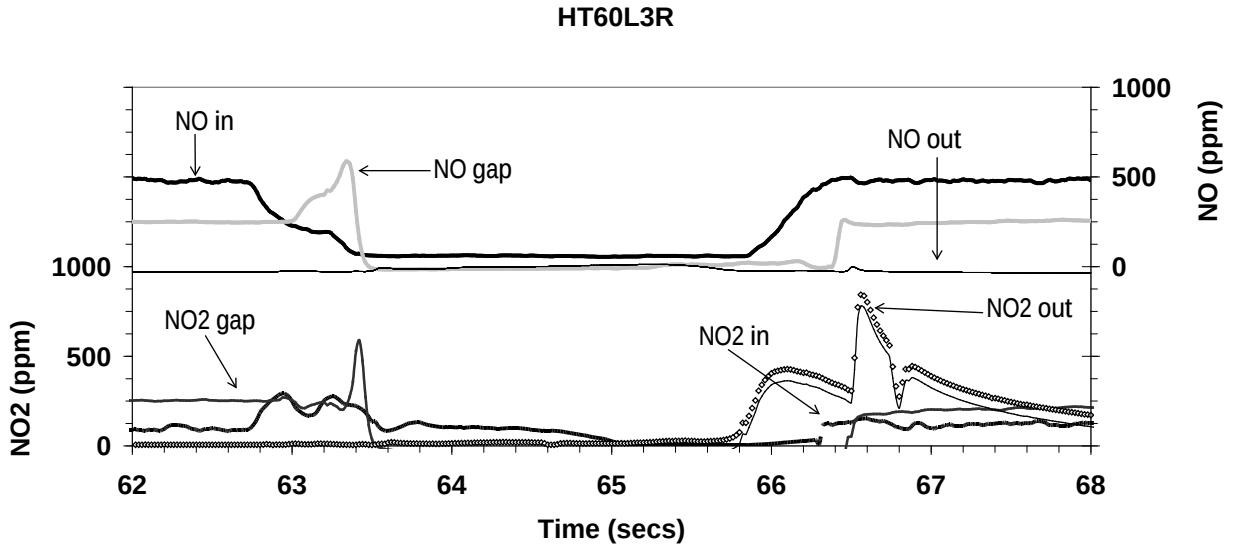

Figure 7(a): HT60L3R – NO and NO_2 emissions during LNT regeneration

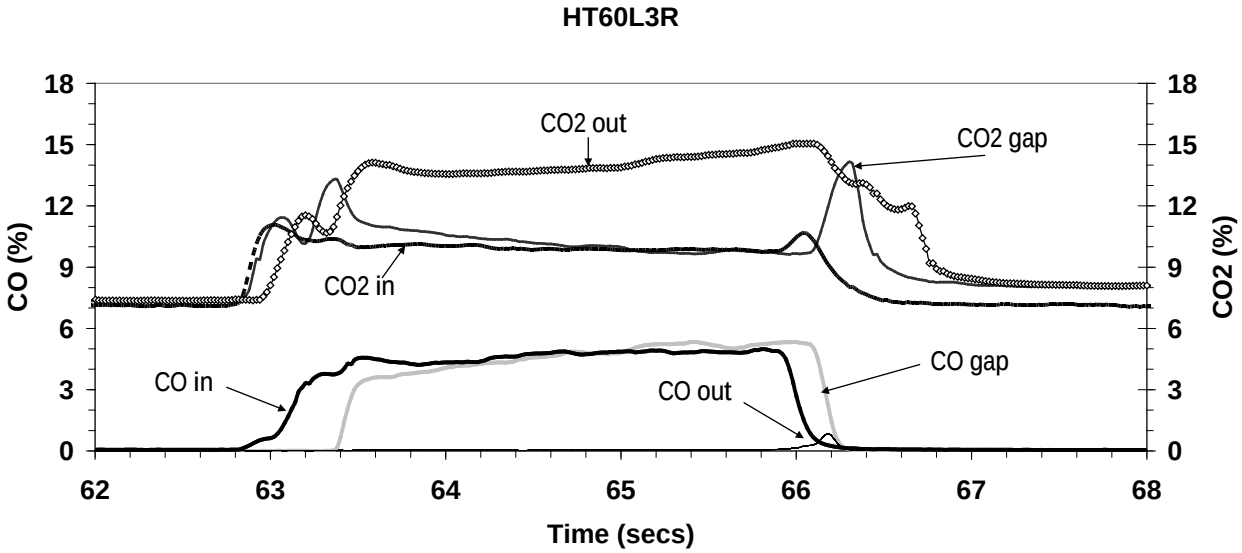

Figure 7(b): HT60L3R – CO and CO_2 emissions during LNT regeneration

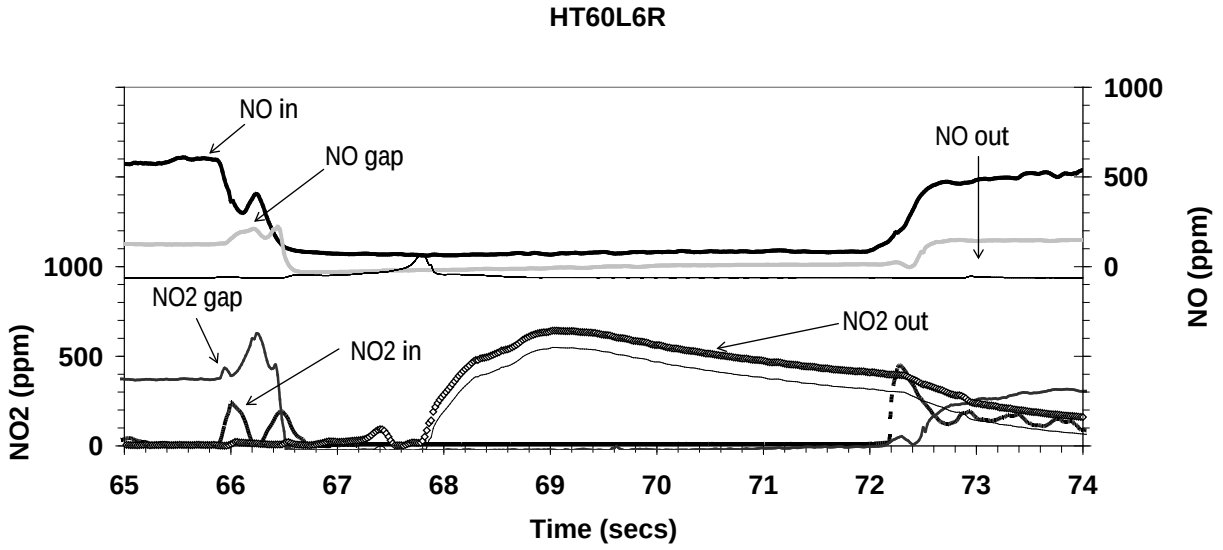

Figure 8(a): HT60L6R – NO and NO_2 emissions during LNT regeneration

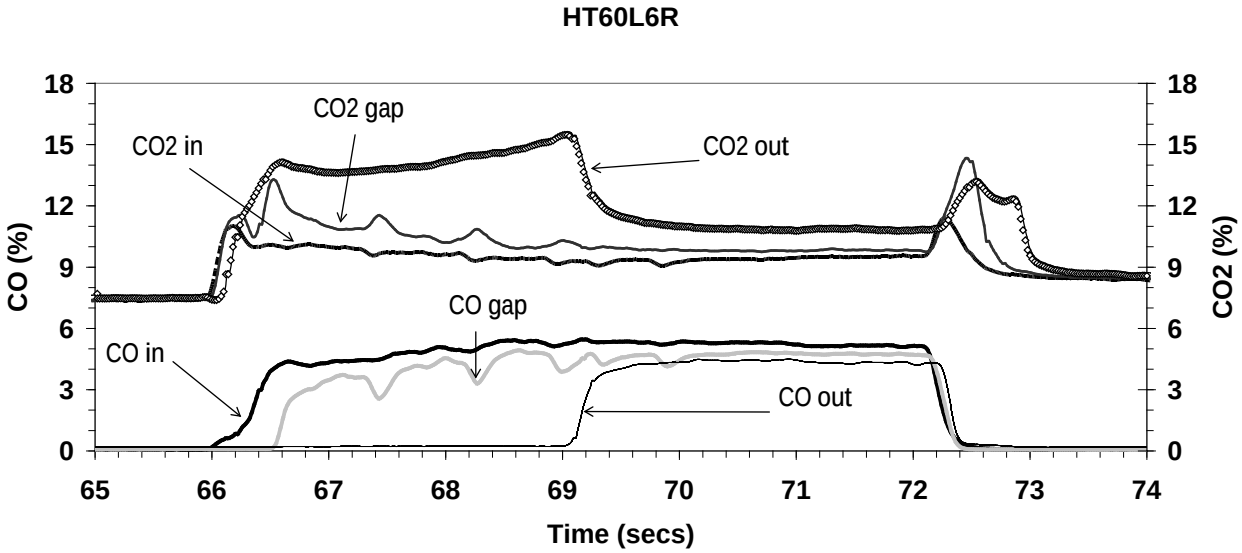

Figure 8(b): HT60L6R – CO and CO_2 emissions during LNT regeneration

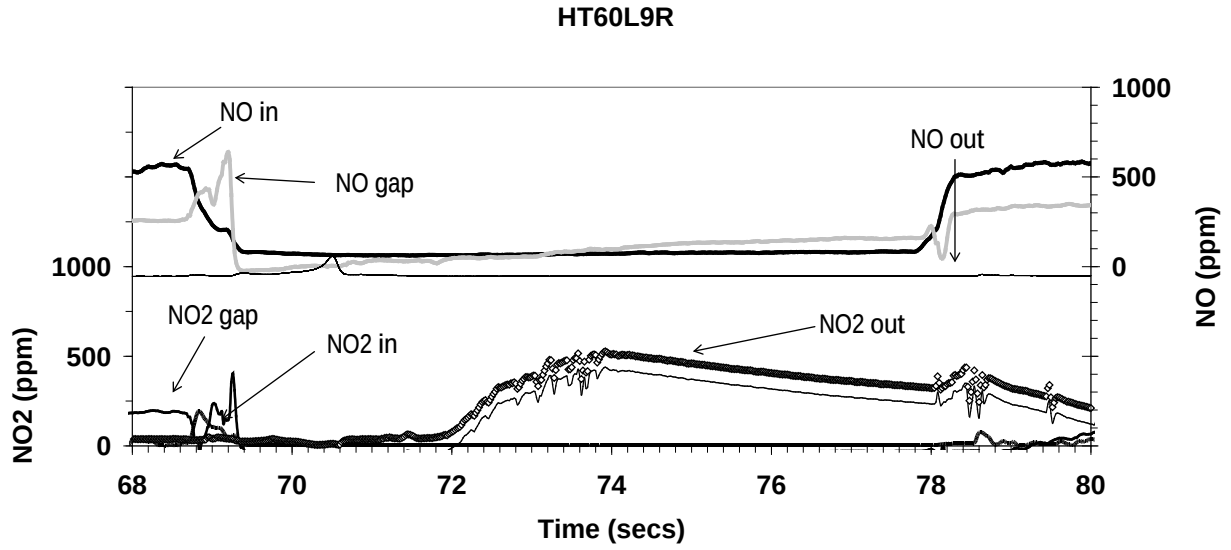

Figure 9(a): HT60L9R – NO and NO_2 emissions during LNT regeneration

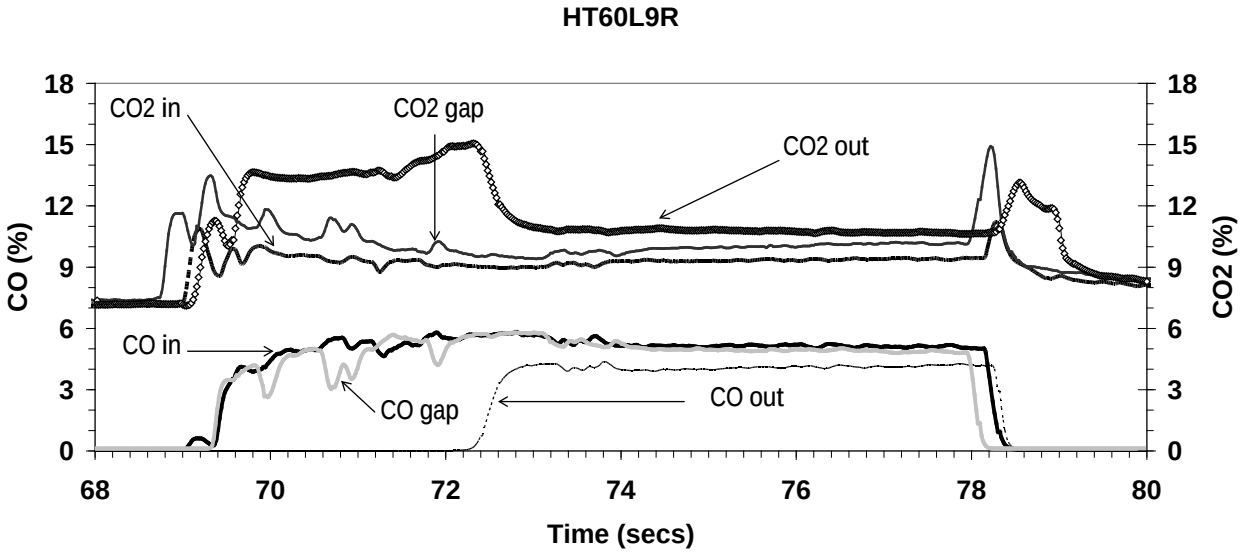

Figure 9(b): HT60L9R – CO and CO_2 emissions during LNT regeneration

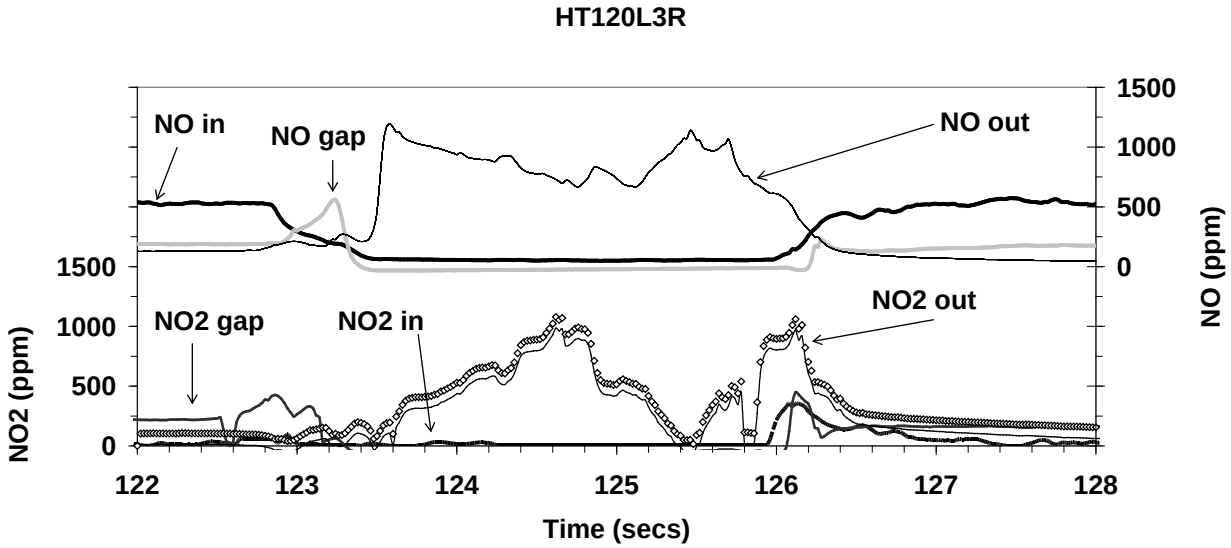

Figure 10(a): HT120L3R – NO and NO_2 emissions during LNT regeneration

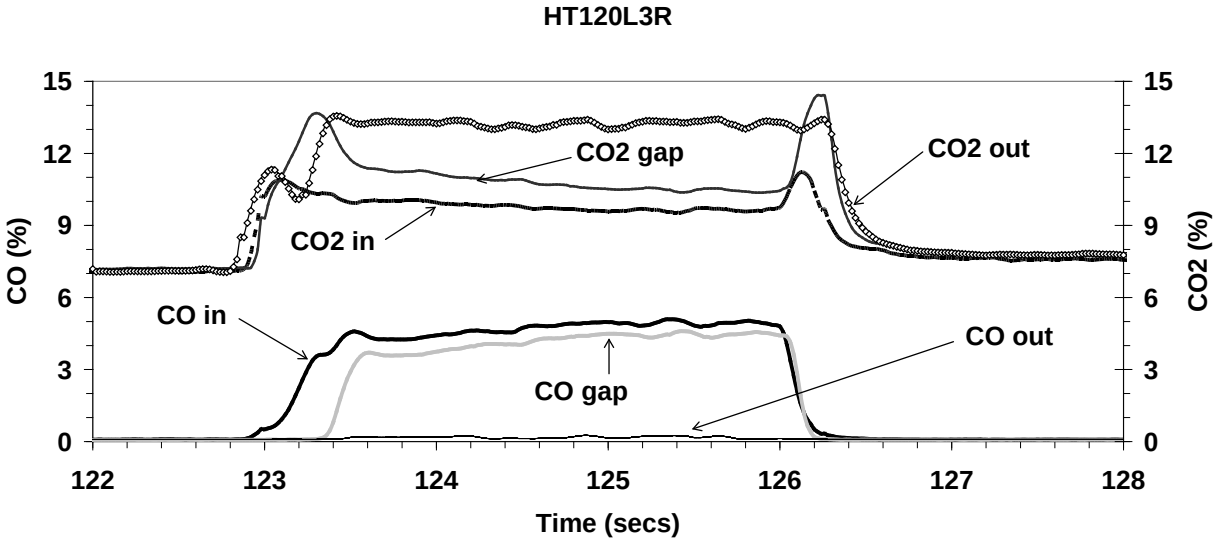

Figure 10(b): HT120L3R – CO and CO_2 emissions during LNT regeneration

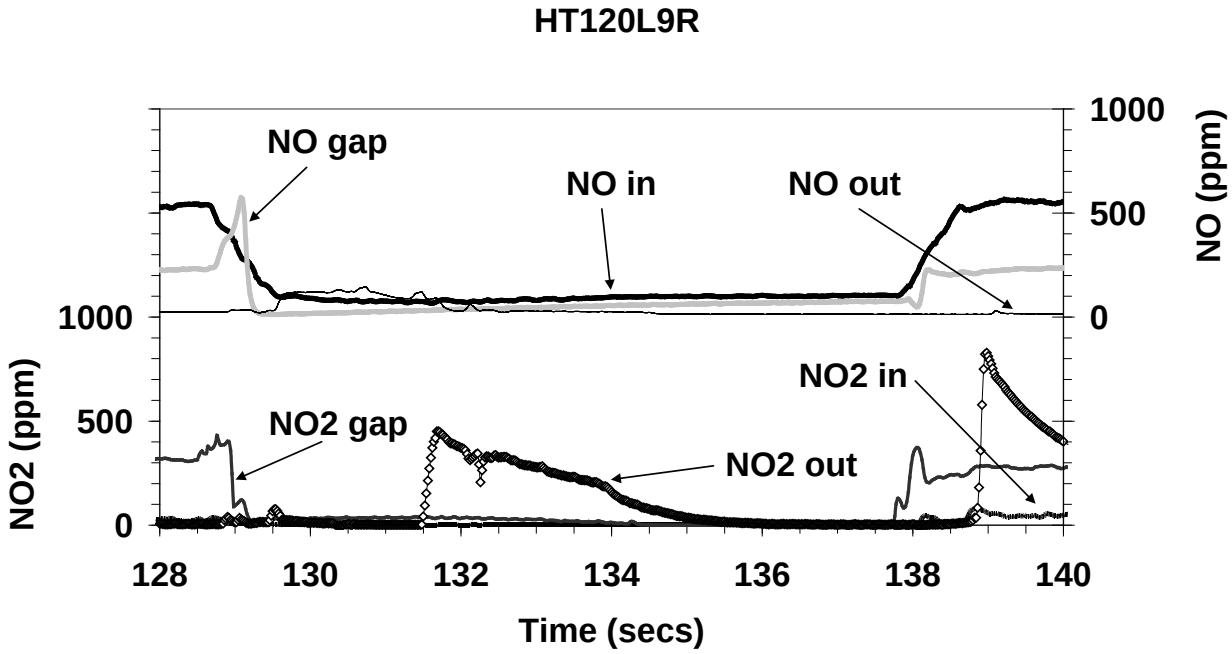

Figure 11(a): HT120L9R – NO and NO_2 emissions during LNT regeneration

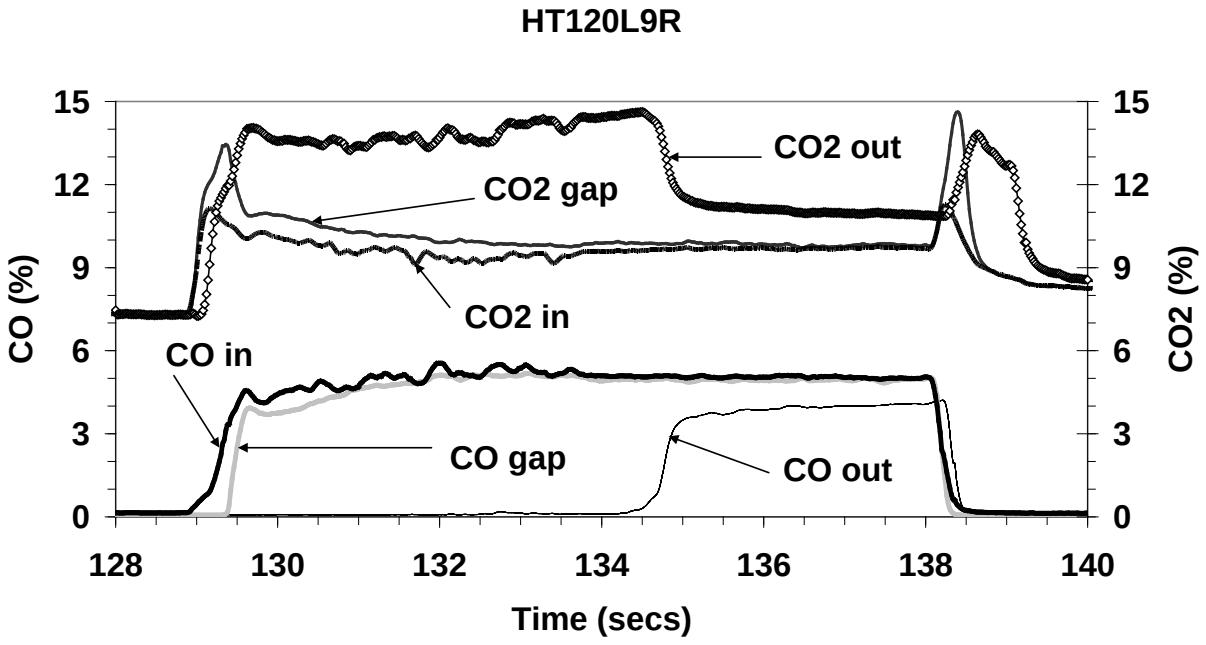

Figure 11(b): HT120L9R – CO and CO_2 emissions during LNT regeneration

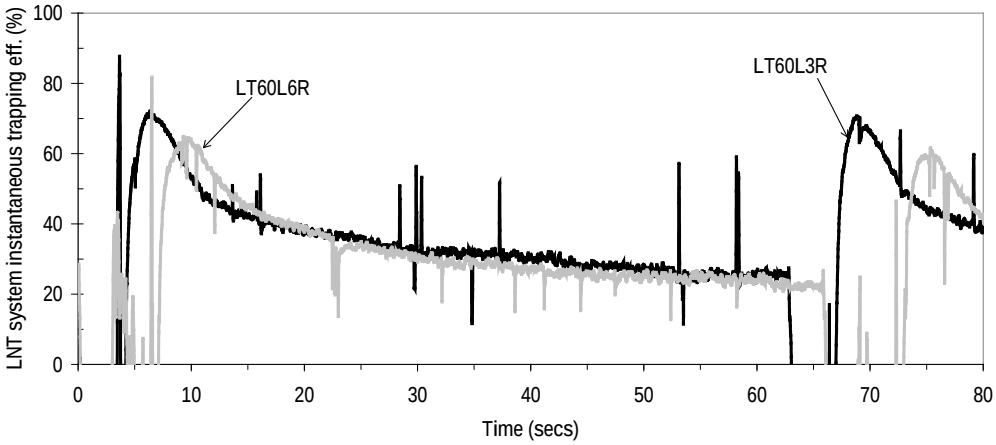

Figure 12(a) – LNT system instantaneous trapping efficiency for low operating temperature: LT60L3R and LT60L6R

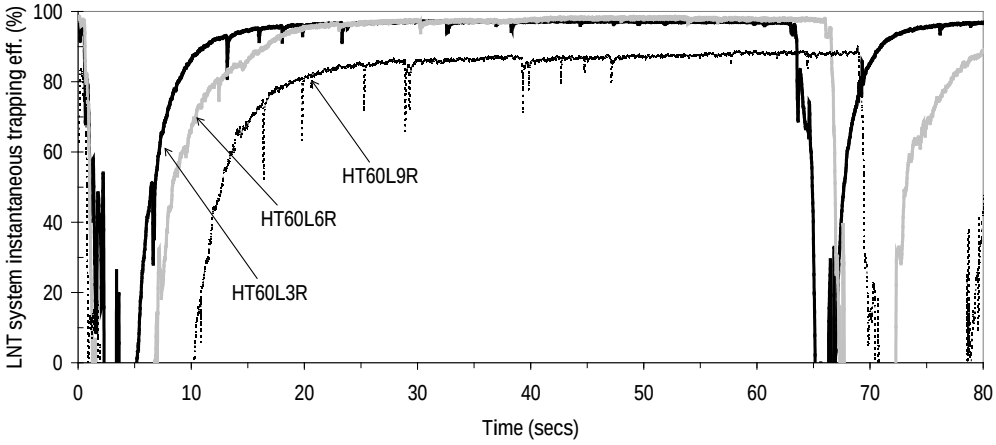

Figure 12(b) – LNT system instantaneous trapping efficiency for high operating temperature: HT60L3R, HT60L6R and HT60L9R

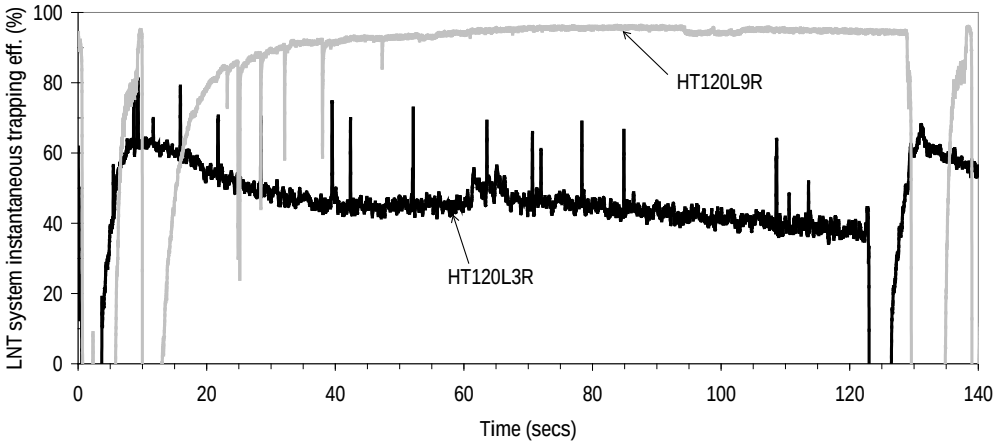

Figure 12(c) – LNT system instantaneous trapping efficiency for high operating temperature: HT120L3R and HT120L9R

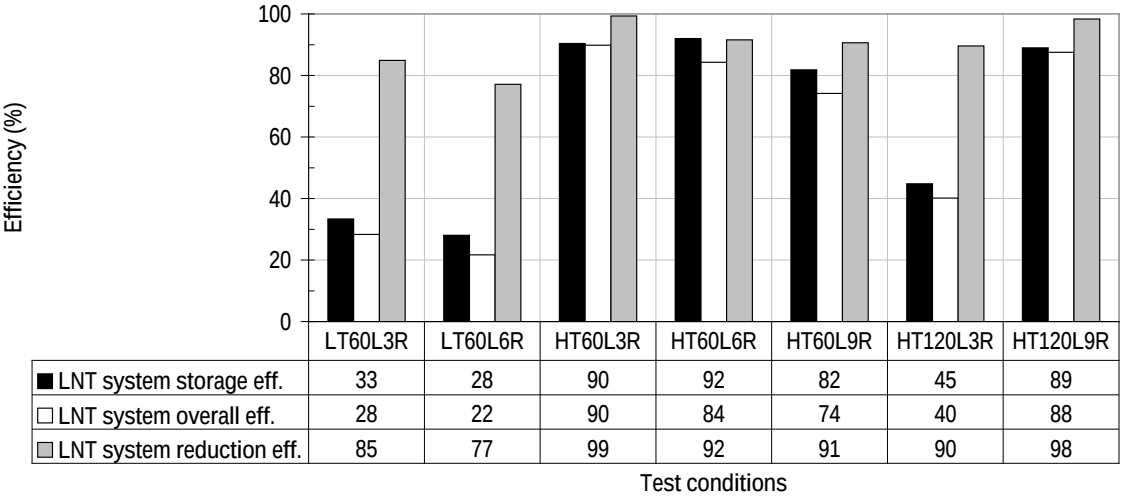

Figure 13 – LNT system: Storage, overall and reduction efficiencies under different test conditions

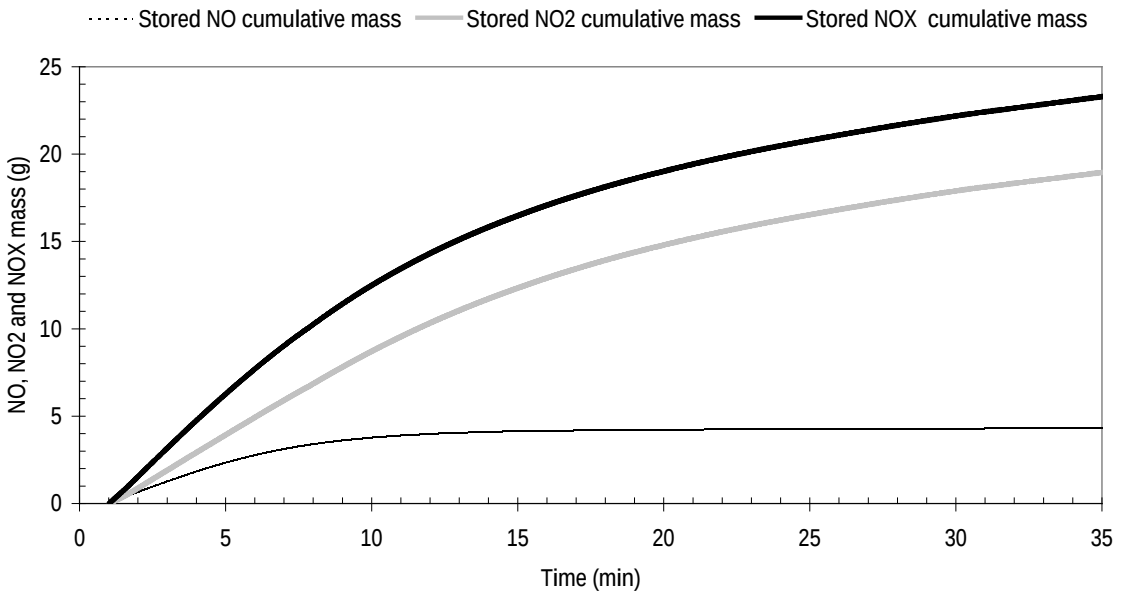

Figure 14: NO_X storage following LNT regeneration at high exhaust temperature